

# Titanium nitride coated tungsten cold field emission sources

W. K. Lo,<sup>a),b)</sup> G. Parthasarathy, C. W. Lo,<sup>a)</sup> D. M. Tanenbaum, H. G. Craighead,  
and M. S. Isaacson

*Applied and Engineering Physics, Cornell University, Ithaca, New York 14853*

(Received 30 May 1996; accepted 17 August 1996)

Titanium nitride (TiN) thin film coatings were studied by field emission microscopy and spectroscopy. Coated tungsten tips were found to be capable of emitting extremely high currents at low extraction voltages ( $\sim 1$  mA at 900–1700 V). Current fluctuations for  $>400 \mu\text{A}$  total emission from a single tip were 7% rms, measured over  $\sim 1$  h. Electron energy distributions measured  $<0.4$  eV (full width at half-maximum). Since TiN thin films are commonly used in the microelectronics industry, TiN coatings have the potential for being a relatively simple and widely accessible method for improving the performance of cold field emission sources. © 1996 American Vacuum Society.

## I. INTRODUCTION

Stable cold field emitters (CFEs) are of interest for vacuum microelectronics device applications because they offer low energy spreads, low power consumption, and high current densities.<sup>1</sup> They can be unstable under poor vacuum and high current conditions, however. This can be addressed by the use of higher strength, more inert, and lower work function materials<sup>2</sup> such as the transition metal carbides and nitrides. This class of materials is interesting because they have conductivities (thermal and electrical) comparable to those of the transition metals while their hardness, inertness, and high melting points are more typical of covalently bonded materials.<sup>3</sup> Promising results obtained using single crystal emitters have been reported by others.<sup>4–7</sup>

For vacuum microelectronics applications, however, emitter fabrication schemes compatible with current thin film processes are required. We therefore studied the emission properties of reactive magnetron sputtered TiN thin films, commonly used as passivation layers and conductive diffusion barriers in integrated circuit technology and as hard, inert coatings for machine tool bits (see Ref. 8, and references therein). High quality films are easily deposited using dc or rf reactive magnetron sputtering systems<sup>9–13</sup> and might be used for coating Mo or Si emitter arrays<sup>1</sup> to improve their performance, or for forming emitter arrays directly (e.g., via a Spindt type process<sup>14</sup>). To make a rapid, preliminary investigation of the field emission properties of TiN coatings we studied TiN thin films deposited onto conventional, electrochemically etched W tips.<sup>15</sup> The field emission behavior of W is well known and provides a good basis for comparison. Stability,  $I$ – $V$  characteristics, current densities, and energy distributions were measured. Transmission electron microscopy (TEM), energy dispersive x-ray (EDX) analysis, and Rutherford backscattering spectroscopy (RBS) were used for film characterization.

## II. EMITTER FABRICATION

W(111) oriented tips were microzone polished using a gold counterelectrode and 6 VDC in a 5% aqueous solution of KOH.<sup>2</sup> Under these conditions, the formed tips were well polished with surfaces smooth down to the nm scale and radii of  $\sim 20$ – $40$  nm, as determined by TEM. After rinsing with distilled water, they were loaded into a dc reactive magnetron sputtering system (CVC 601) with their points towards the target. After evacuating to a base pressure of  $\sim 7 \times 10^{-8}$  Torr, the tips were lightly sputtered using  $\text{Ar}^+$  (300 V, 300 mA) for  $\sim 2$  min to remove any surface contaminants. For this short sputtering time (actual time  $<30$  s, due to turntable rotation) and low energy, no significant tip roughening was observed in the TEM micrographs. The Ti target (99.9% pure, 8 in. diameter) was cleaned by presputtering under the deposition conditions for 5 min. TiN was then deposited onto the tips for 5 min. The deposition conditions were 2 kW regulated power, 3.4 mTorr chamber pressure, 10/16 sccm flow rates for  $\text{Ar}/\text{N}_2$ , and 20 rpm turntable rotation rate. Afterwards, coated tips were transferred through air to a field emission test system<sup>2</sup> where they were baked in its load lock (base pressure  $\sim 1 \times 10^{-8}$  Torr at  $\sim 150$  °C for  $\sim 2$  h to degas water vapor. Inside the main chamber, tips were processed by voltage cycling as follows. With no heating and starting with no emission, the extraction voltage was ramped up in 25 V steps every 2 s until the emission current reached or exceeded a preset limit (initially,  $5 \mu\text{A}$ ). After 2 s, the voltage was ramped back to its initial value. This cycle was repeated with the current limit approximately doubled each time. A maximum limit of  $\sim 1$  mA was arbitrarily imposed. Tips processed in this way tended to emit over relatively large solid angles from randomly dispersed emission sites (see Fig. 2).

## III. EMITTER CHARACTERIZATION

The deposited films had the gold color characteristic of TiN<sup>16</sup> RBS analysis of films deposited onto flat, glassy carbon substrates<sup>17</sup> indicated a 1:1 Ti:N ratio with  $\sim 5$ – $10\%$  O incorporation throughout. EDX analysis was performed on tips using an ultrahigh vacuum (UHV) scanning TEM (STEM) after field emission testing. Difficulties with speci-

<sup>a)</sup>Present address: Schlumberger Technologies—ATE Division, 1601 Technology Dr., San Jose, CA 95110.

<sup>b)</sup>Electronic mail: wklo@san-jose.ate.slb.com

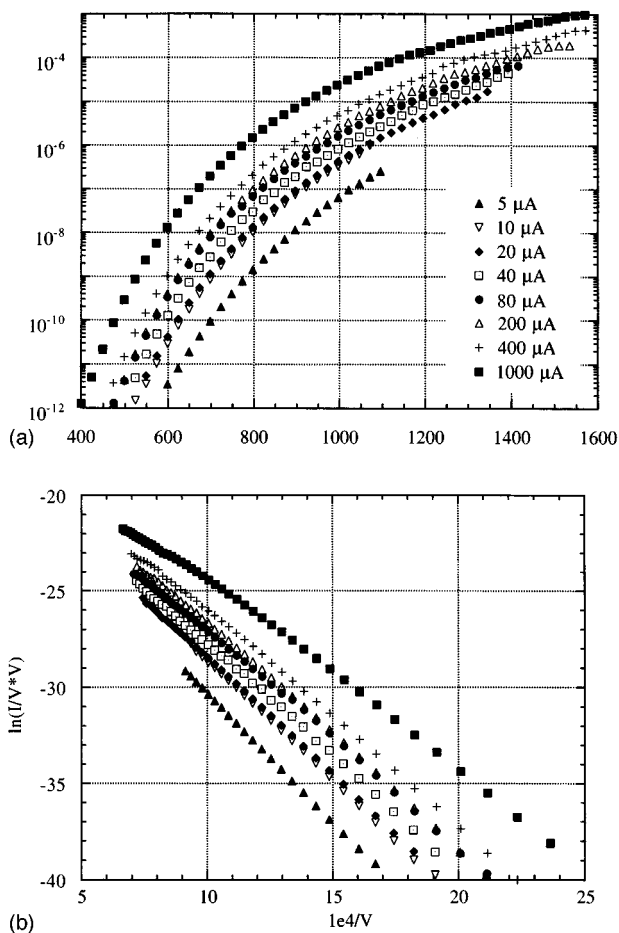


FIG. 1. (a)  $I$ - $V$  data taken from one tip during voltage cycling. As shown, the emission current generally increases after cycling to the next higher limit (plot legend). A total increase of more than two orders of magnitude is indicated. Vertical and horizontal axes units are amps and volts, respectively. (b) Fowler-Nordheim plots for the  $I$ - $V$  data shown in (a). Slopes and intercepts obtained by least-squares fitting are given in Table I. Units are consistent with Eqs. (1) and (2).

men preparation prevented chemical analysis at the apex of the tip. Analysis of the shank portion verified the presence of both titanium and nitrogen. TEM of coated tips was used to determine film thickness and morphology. For the conditions above, the deposition rate was found to be 22 nm/min. Films were very fine grained ( $< \text{few nm}$ ) and corresponding diffraction patterns consisted of diffuse, concentric rings, typical of polycrystalline specimens.<sup>18</sup> Occasionally, a few ( $\sim 10$ ) small ( $\sim 5$  nm radii) asperities could be found at the film surface near the tip apex. These asperities had an areal density of  $\sim 10^{-4}$  nm<sup>2</sup>. Otherwise, the films appeared smooth on the nm scale.

#### IV. RESULTS/DISCUSSIONS

Figure 1(a) shows  $I$ - $V$  data for one tip undergoing the voltage cycling procedure. It was recorded during the decreasing portion of each cycle, after the current had reached the indicated limits. As shown, emission for a given voltage tended to increase after each voltage cycle. These increases

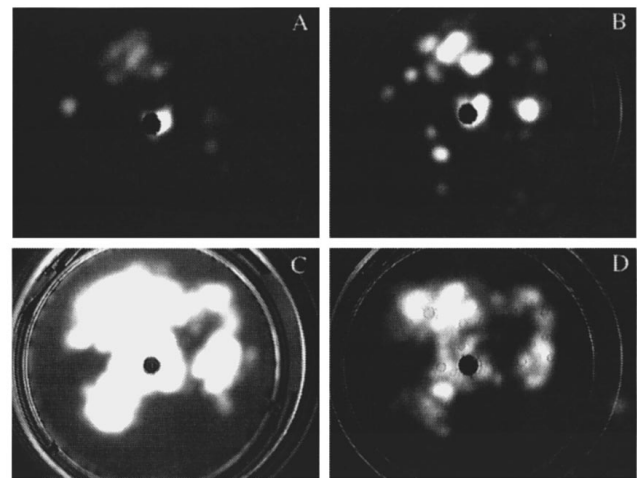


FIG. 2. Field emission patterns taken during voltage cycling. (A)–(C) Taken under the same video exposure conditions. (D) Same as (C) except for a  $16\times$  reduction in exposure time to better show the pattern details. (A) Image at  $\sim 1300$  V with  $\sim 5$   $\mu$ A of emission; (B) imaged at  $\sim 1300$  V with  $\sim 40$   $\mu$ A of emission; and (C) and (D) were imaged at  $\sim 1600$  V with  $\sim 700$   $\mu$ A of emission. The dark central region in these images is the probe hole aperture holder in the phosphor screen. The crescent shaped structure in (A) and (B) is a portion of the field defining aperture and results from a slight misalignment of the tip [corrected for in (C) and (D)].

occurred abruptly, usually within one or two voltage steps during the upward portion of the cycle. Total increases of greater than two orders of magnitude were measured after conditioning to 1 mA. Corresponding emission patterns imaged after voltage cycling to 5  $\mu$ A, 80  $\mu$ A, and 1 mA are shown in Figs. 2(A)–2(C), respectively. Figure 2(D) is identical to Fig. 2(C) except for an effective reduction in exposure time to better show the pattern details. For this particular tip, no extensive changes in these emission patterns were observed indicating that there were no extensive tip geometry changes. Also, no evidence of emission from multiple asperities was found. These asperities tend to result in emission patterns consisting of a few large, overlapping emission lobes. Extensive field emission pattern changes and evidence for multiple asperity (2–4) emission have been observed for some TiN/W tips, particularly those emitting at the lowest extraction voltages.

After conditioning, TiN/W tips were found to be capable of extremely high current emission at low extraction voltages ( $\sim 1$  mA at 900–1700 V). For comparison, clean W tips typically emit only  $\sim 10$   $\mu$ A at extraction voltages of a few kV. Corresponding angular current densities were as high as 500  $\mu$ A/sr ( $> 50$  nA through the screen probe hole) which approaches that available from Zr/O/W Schottky emitters<sup>19</sup> and is very much greater than is possible from pure W ( $\sim \text{few } \mu\text{A/sr}$  at 1 kV).<sup>2</sup> Even considering emission from multiple (2–4) asperities, these TiN/W tips are superior to uncoated W tips. Measurements made on W(111) tips emitting from multiple asperities [formed by high energy (60 keV) Au<sup>+</sup> ion milling<sup>20</sup>] indicate that only up to a few tens of  $\mu$ A emission current (at  $\sim 500$ –1000 V) can be drawn before tip destruction occurs. This suggests that emission

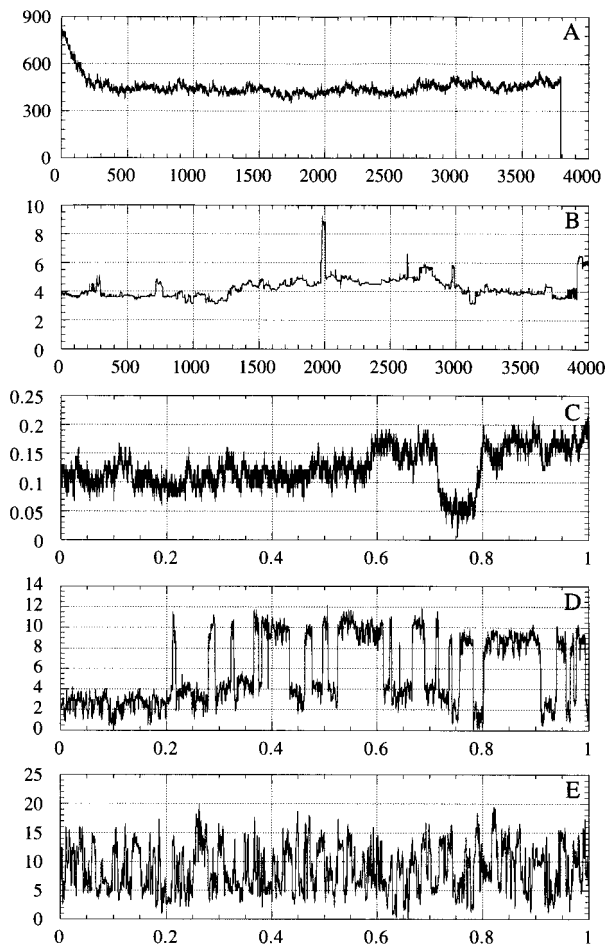


FIG. 3. (A) Emission stability for a single tip emitting  $>400 \mu\text{A}$  at 1600 V. (B) Stability under low current conditions ( $\sim\text{few } \mu\text{A}$  at 650 V). (C)–(E) The ac current fluctuations for 25, 200, and 500  $\mu\text{A}$  of total emission current at 635, 811, and 936 V extraction voltage, respectively. The current fluctuations increase in frequency with increasing current. Vertical axes for all plots are  $\mu\text{A}$ . Horizontal units for (A) and (B) are s. Horizontal units for (C)–(E) are  $\mu\text{s}$ .

from multiple asperities cannot be solely responsible for the high emission currents reported here.

Emission stability for the tip shown in Fig. 2, taken while emitting an average current  $>400 \mu\text{A}$  at 1600 V, is shown in Fig. 3(A). Neglecting the initial decay, the current fluctuations (measured at a rate of 1 Hz over  $\sim 1$  h. with  $\sim 20$  ms resolution) were  $\sim 7\%$  rms. The initial decay is characteristic of the effects of recontamination from the ambient after tip flashing (cleaning by heating for short periods). This strongly suggests that at least part of the observed current increases is due to tip cleaning, possibly by Joule heating by the high emission currents. Other possible origins are discussed below. The rapidity of the decay may be due to degradation of the local vacuum conditions caused by the high current flux on the phosphor screen with a resultant increase in the electron stimulated desorption rate of contaminants or in the phosphor decomposition rate.<sup>1</sup>

Somewhat surprisingly, operation at low emission levels ( $\sim 10 \mu\text{A}$ ) did not necessarily improve medium term emis-

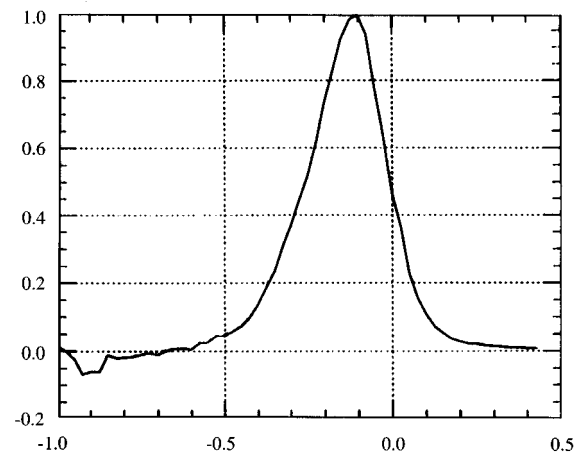


FIG. 4. Typical field emission energy distribution for TiN/W tips. For this distribution, the angular current density was  $\sim 24 \mu\text{A}/\text{sr}$  at 1.5 kV. The vertical axis has an arbitrary scale whereas the horizontal axis has units of eV on a relative scale.

sion stability (over a few hours). Abrupt current jumps often became more pronounced and resulted in a decrease in stability [Fig. 3(B)]. These jumps were found to coincide with intensity fluctuations of individual emission sites and are possibly due to adsorbate coverage changes.<sup>21</sup> The rate at which these fluctuations (screen intensity and emission current) occurred increased dramatically with increasing emission [Figs. 3(C) to 3(E)]. We speculate that fluctuations occurring at different emission sites are not correlated and average out under high current conditions, resulting in the improved stability observed.

Energy measurements for angular current densities as high as  $\sim 35 \mu\text{A}/\text{sr}$  at 1 kV, indicate full width at half-maximums (FWHMs) of 0.3–0.4 eV (Fig. 4). This is comparable to the distributions measured for clean W (0.2–0.4 eV). Spectrometer limitations prevented analysis at higher densities. Except for the nearly symmetrical shape of the distribution, it is mostly characteristic of emission from a free electron system (i.e., no discernible band structure or resonant tunneling effects). The symmetry of the distribution appears to be a real feature for this system and not a result of analyzer misalignment.<sup>22</sup> It was reproducible for the various TiN tips tested and was not observed for distributions measured from clean W. Its origin has not yet been identified.

To analyze the field emission data taken during voltage cycling, we turn to Fowler–Nordheim (FN) theory.<sup>23–25</sup> The FN equation for planar field emission is well known and can be written, after suitable approximations (see Ref. 1, for example) as

$$I = aV^2 \exp(-b/V), \quad (1)$$

where

$$a = 1.4 \times 10^{-6} \frac{\alpha\beta^2}{\phi} \exp\left(\frac{9.8}{\sqrt{\phi}}\right)$$

and

$$b = 6.5 \times 10^7 \frac{\phi^{3/2}}{\beta}. \quad (2)$$

$I$ (A) is the tip emission current,  $V$ (V) is the extraction voltage,  $\phi$  (eV) is the work function,  $\alpha$  (cm<sup>2</sup>) is the effective emission area, and  $\beta$  (1 cm) is the field conversion factor. An experimental plot of  $\ln(I/V^2)$  vs  $1/V$  is thus expected to yield a straight line with the slope and intercept giving  $\ln(a)$  and  $-b$ , respectively. If the work function is assumed to lie in the range between 3.4 and 11.6, it can be shown using Eqs. (2) that the emission area is approximately given by

$$\alpha = ab^2 / (1.34 \times 10^{13}) (\text{cm}^2), \quad (3)$$

accurate to  $\pm 10\%$ .<sup>1</sup>

Deviations of the FN plots from the expected linear behavior can occur at high currents due to space charge effects and/or emission from sharp microprotrusions. Considering the high emission currents drawn, space charge effects may be present for the data plotted in Fig. 1(a), particularly at the highest currents where some deviation from linearity is observed [Fig. 1(b)]. Space charge does not affect the FN analysis if the linear portion of the data is used for fitting.<sup>26</sup> Field emission from microprotrusions does not necessarily obey FN behavior due to a breakdown of the planar emission assumption.<sup>27</sup> In this case,  $\alpha$  and  $\beta$  may not have simple relationships to actual physical quantities such as the emission area or tip shape, but must be thought of as fitting parameters. To avoid this complication, data from a tip that showed no evidence of emission from tip asperities (see discussion above) were purposely chosen for this analysis. For tips showing clear evidence of emission from tip asperities, FN plots deviated significantly from linearity, even at moderate emission currents.

From Eqs. (1) and (2), possible origins for the current increases observed during voltage cycling are (i) a reduction of the emitter radius of curvature during operation. This might result from emitter sharpening by backsputtering by ionized residual gases<sup>1</sup> or by field assisted surface migration.<sup>28</sup> This seems unlikely, however, due to the self-limiting nature of the current increases.<sup>7</sup> Emitter sharpening by either mechanism would likely continue until tip destruction. (ii) An increase in the active emission area, due, perhaps, to removal of insulating oxide layers. Thin surface oxide layers, consisting mainly of TiO<sub>2</sub>, are known to form on TiN.<sup>29,30</sup> (iii) A decrease of the tip work function via desorption of electronegative species (e.g., O).<sup>1</sup> Oxygen adsorption on TiN films has been observed using x-ray photoelectron spectroscopy by others.<sup>29</sup> Origins (ii) and (iii) will be examined below.

Fits to the linear portions of the data in Fig. 1(b) yield the FN slopes and intercepts given in Table I. Effective emission areas calculated using Eq. (3) are also given. As shown, some increase in the effective emission area occurs during voltage cycling. The exact amount appears to be tip dependent. For certain tips, the emission area increase is more consistent with the observed current increases. For others,

TABLE I. Fowler–Nordheim fitting parameters and estimated emission areas from Fig. 1(b).

| Current limit<br>( $\mu$ A) | $a$                   | $b$                | Emission area $\alpha$<br>(cm <sup>2</sup> ) |
|-----------------------------|-----------------------|--------------------|--|
| 5                           | $4.18 \times 10^{-8}$ | $1.34 \times 10^4$ | $5.6 \times 10^{-13}$                        |
| 10                          | $9.40 \times 10^{-8}$ | $1.24 \times 10^4$ | $11 \times 10^{-13}$                         |
| 20                          | $7.85 \times 10^{-8}$ | $1.21 \times 10^4$ | $10 \times 10^{-13}$                         |
| 40                          | $9.49 \times 10^{-8}$ | $1.16 \times 10^4$ | $9.6 \times 10^{-13}$                        |
| 80                          | $10.6 \times 10^{-8}$ | $1.11 \times 10^4$ | $9.8 \times 10^{-13}$                        |
| 200                         | $39.7 \times 10^{-8}$ | $1.18 \times 10^4$ | $41 \times 10^{-13}$                         |
| 400                         | $52.5 \times 10^{-8}$ | $1.14 \times 10^4$ | $51 \times 10^{-13}$                         |
| 1000                        | $70.2 \times 10^{-8}$ | $1.01 \times 10^4$ | $53 \times 10^{-13}$                         |

however, such as the one discussed here, the calculated increases cannot fully account for the more than two orders of magnitude current gains.

If it is assumed that tip shape (i.e.,  $\beta$ ) changes are negligible (a reasonable assumption based on the small field emission image changes observed, Fig. 2), work function changes can be investigated using the FN slope relationship in Eqs. (2). Small changes in work function are given by

$$\frac{\Delta \phi}{\phi} = \frac{2}{3} \frac{\Delta b}{b}. \quad (4)$$

From the data in Table I, an  $\sim 20\%$  change in work function is indicated. This suggests that decreasing work function values are also partly responsible for the current increases observed.

## V. CONCLUSIONS

The field emission properties of reactive magnetron sputtered TiN on W tips were studied. For a rapid, preliminary evaluation, films were deposited onto conventional, electrochemically etched W tips. They were characterized using a variety of techniques including TEM, RBS, and EDX. For these tips, significant emission current gains resulted from a simple voltage cycling procedure. After undergoing this procedure, tips were found to be capable of emitting extremely high currents at low voltages (1 mA at 900–1600 V) that is orders of magnitude greater than possible from uncoated W at similar extraction voltages. Fowler–Nordheim analysis of  $I$ – $V$  data suggests that the observed current increases are due to work function decreases as well as to active emission area increases. Tip self-cleaning by Joule heating may play a role as well. Energy distributions measured up to  $\sim 35 \mu\text{A}/\text{sr}$  at 1 kV had  $< 0.4$  eV FWHM. TiN coatings have the potential to be an economical method for making or improving the performance of cold field emission sources for vacuum microelectronic device applications.

## ACKNOWLEDGMENTS

The authors thank M. Y. Lanzerotti and Professor A. Gaeta for the loan of their sampling oscilloscope. They are grateful to Professor M. Thompson for his assistance with the RBS analysis, to J. Drumheller for his assistance with reactive magnetron sputtering, and to M. Thomas for his EDX analysis. This work was supported by ARPA Grant No.

F49620-93-C-0061. It made use of the Cornell Nanofabrication Facility which is partially supported by the National Science Foundation under Award No. ECS-8619040 and the MRL Central Facilities supported by the National Science Foundation under Award No. DMR-9121654.

- <sup>1</sup>I. Brodie and C. A. Spindt, in *Advances in Electronics and Electron Physics: Microelectronics and Microscopy*, edited by P. W. Hawkes (Academic, New York, 1992), Vol. 83, p. 1.
- <sup>2</sup>W. K. Lo, M. Skvarla, C. W. Lo, H. G. Craighead, and M. S. Isaacson, *J. Vac. Sci. Technol. B* **13**, 2441 (1995).
- <sup>3</sup>L. E. Toth, *Transition Metal Carbides and Nitrides* (Academic, New York, 1971), Vol. 7.
- <sup>4</sup>Y. Ishizawa, T. Aizawa, and S. Otani, *Appl. Surf. Sci.* **67**, 36 (1993).
- <sup>5</sup>M. L. Yu, B. W. Hussey, T. H. P. Chang, and W. A. Mackie, *J. Vac. Sci. Technol. B* **13**, 2436 (1995).
- <sup>6</sup>W. A. Mackie, R. L. Hartman, and P. R. Davis, *Appl. Surf. Sci.* **67**, 29 (1993).
- <sup>7</sup>W. A. Mackie, R. L. Hartman, M. A. Anderson, and P. R. Davis, *J. Vac. Sci. Technol. B* **12**, 722 (1994).
- <sup>8</sup>S. Inoue, H. Uchida, K. Takeshita, K. Koterazawa, and R. P. Howson, *Thin Solid Films* **261**, 115 (1995).
- <sup>9</sup>F. Elstner, A. Ehrlich, H. Giegengack, H. Kupfer, and F. Richter, *J. Vac. Sci. Technol. A* **12**, 476 (1994).
- <sup>10</sup>W. D. Sproul and R. Rothstein, *Thin Solid Films* **126**, 257 (1985).
- <sup>11</sup>U. Kopacz and H. A. Jehn, *Thin Solid Films* **126**, 265 (1985).
- <sup>12</sup>B. O. Johansson, J.-E. Sundgren, J. E. Greene, A. Rockett, and S. A. Barnett, *J. Vac. Sci. Technol. A* **3**, 303 (1984).
- <sup>13</sup>M. Milic, M. Milosavljevic, N. Bibic, and T. Nenadovic, *Thin Solid Films* **126**, 319 (1985).
- <sup>14</sup>C. A. Spindt, I. Brodie, L. Humphrey, and E. R. Westerberg, *J. Appl. Phys.* **47**, 5248 (1976).
- <sup>15</sup>J. Ishikawa, H. Tsuji, Y. Gotoh, T. Sasaki, and T. Kaneko, *J. Vac. Sci. Technol. B* **11**, 403 (1993).
- <sup>16</sup>G. Reiners, U. Beck, and H. A. Jehn, *Thin Solid Films* **253**, 33 (1994).
- <sup>17</sup>Alfa Aesar, Johnson-Matthey Catalog Co., 30 Bond St., Ward Hill, MA 01835-9953.
- <sup>18</sup>R. H. Alderson and J. S. Halliday, in *Techniques For Electron Microscopy*, edited by D. Kay (Blackwell Scientific, Oxford, 1965), p. 473.
- <sup>19</sup>D. W. Tuggle and L. W. Swanson, *J. Vac. Sci. Technol. B* **3**, 220 (1984).
- <sup>20</sup>Unpublished results.
- <sup>21</sup>L. W. Swanson, *Surf. Sci.* **70**, 165 (1977).
- <sup>22</sup>J. Unger, Y. A. Vlasov, and N. Ernst, *Appl. Surf. Sci.* **87/88**, 45 (1995).
- <sup>23</sup>R. H. Fowler and L. Nordheim, *Proc. R. Soc. London Ser. A* **119**, 173 (1928).
- <sup>24</sup>L. W. Nordheim, *Proc. R. Soc. London Ser. A* **121**, 626 (1928).
- <sup>25</sup>R. H. Good and E. W. Müller, in *Encyclopedia of Physics*, edited by S. Flügge (Springer, Berlin, 1956), Vol. 21.
- <sup>26</sup>R. Gomer, *Field Emission and Field Ionization* (AIP, New York, 1993).
- <sup>27</sup>P. H. Cutler, J. He, and N. M. Miskovsky, *J. Vac. Sci. Technol. B* **11**, 387 (1993).
- <sup>28</sup>M. S. Mousa, P. R. Schwoebel, I. Brodie, and C. A. Spindt, *Appl. Surf. Sci.* **67**, 56 (1993).
- <sup>29</sup>L. Porte, L. Roux, and J. Hanus, *Phys. Rev. B* **28**, 3214 (1983).
- <sup>30</sup>M. J. Vasile, A. B. Emerson, and F. A. Baiocchi, *J. Vac. Sci. Technol. A* **8**, 99 (1990).